Melting of lead under high pressure studied using second-scale time-resolved x-ray diffraction

Agnès Dewaele,[1] Mohamed Mezouar,[2] Nicolas Guignot,[2,*] and Paul Loubeyre[1]
[1]*DIF/Département de Physique Théorique et Appliquée, CEA, Boîte Postale 12, 91680 Bruyères-le-Châtel, France*
[2]*European Synchrotron Radiation Facility, Boîte Postale 220, F-38043 Grenoble Cedex, France*
(Received 13 April 2007; revised manuscript received 20 August 2007; published 16 October 2007)

The high pressure and high temperature phase diagram of lead has been studied up to 80 GPa and 3700 K in a laser-heated diamond anvil cell. Melting and solid-solid phase transitions have been followed with a second scale by *in situ* synchrotron time-resolved x-ray diffraction. The detection of the x-ray signal scattered by the liquid was used as an objective criterion for melting. We evidenced that the melting phenomenon in a diamond anvil cell has a typical lifetime that can be as low as 1 s. Unlike a previous laser-heated diamond anvil cell study, the measured melting curve is in agreement with melting points detected using dynamic compression and confirms the predictions of *ab initio* calculations. The pressure-temperature conditions of the hcp-bcc phase transition have been measured, and the hcp-bcc-liquid triple point has been located around 39 GPa and 2400 K.

DOI: 10.1103/PhysRevB.76.144106 PACS number(s): 62.50.+p, 07.35.+k, 61.10.Eq, 64.30.+t

I. INTRODUCTION

The thermodynamic conditions and microscopic process of melting of the elements under high pressure is of great interest to fields spanning from fundamental physics—to detect changes in chemical bonds in the solid or liquid phases in extreme conditions[1]—to planetary interior's study—to better constrain their thermal models.[2] Three independent approaches have been used to study melting lines under pressure: (i) the optically detected melting in laser-heated diamond anvil cell (o-LHDAC), (ii) the melting induced by shock-wave (SW) compression, and (iii) the *ab initio* calculations of the liquid-solid equilibrium conditions. A good agreement was obtained between o-LHDAC, SW, and calculations for some systems such as aluminum or copper.[3,4] However, puzzling discrepancies between melting lines determined by these approaches have been reported for several other systems, the general trend being that o-LHDAC melting curves are lower than both shock and *ab initio* melting curves. New models of melting have been proposed to explain the observed differences between static and dynamic melting points (for tantalum,[5,6] lead,[7,8] iron,[2,9] molybdenum,[5] etc.): in particular, superheating-melting behaviors of shocked solids, which deviate from equilibrium melting.[10,11] However, these models failed in explaining the difference between iron SW and o-LHDAC melting[10] (which differ by approximately 1000 K at 200 GPa). Moreover, recent *ab initio* calculations confirmed the SW melting points of both iron[12] and tantalum[13] and predicted a melting line of lead significantly higher than o-LHDAC measurements.[14] The accuracy of the o-LHDAC approach has thus been questioned; its major drawback is the criterion used for melting, which is based on the detection of the changes of the optical properties of the surface of the laser-heated sample.[2,7] This criterion does not allow distinguishing if these changes are caused by the melting or by structural changes in the sample,[15,16] in the pressure transmitting medium, or in both in case of chemical reactions.[17] X-ray diffraction has been often used to detect melting and to study the melt structure in the case of resistive heated diamond-anvil cell (DAC),[18] or large volume presses,[19] but these techniques reach a limited pressure-temperature range. Recently, Shen *et al.*[20] showed that this diagnostic—the recording of an x-ray pattern characteristic of a liquid sample—could be used in LHDAC. In this study, it was pointed out that a criterion proposed before—the disappearance of the signal diffracted by the solid sample[6]—was not reliable. However, the difficulties of such measurements, with the x-ray technique used, allowed Shen *et al.* to measure only four melting points for iron up to 58 GPa.[20] After numerous attempts to reproduce these measurements with similar techniques, we reduced the x-ray diffraction detection time by an order of magnitude, down to $\simeq$2 s. This time scale was chosen to be able to fully characterize the rapid crystallographic changes and melting in the laser-heated sample, which could be inferred from the observation of its shape evolution. We show in this paper that this technique, named x-LHDAC, is a major improvement over both o-LDAC[2] and previous x-ray detection based melting studies.[6,20] Lead is chosen as a test case to investigate whether this improved criterion could resolve the static-dynamic discrepancy on the temperature of melting, which has been reported to reach 800 K at only 50 GPa for this element.[8]

II. EXPERIMENTAL METHODS AND OBSERVATIONS

We used the laser-heating system of the ID27 beamline at the European Synchrotron Radiation Facility.[21,22] Four experimental runs have been carried out. Membrane diamond anvil cells equipped with 200–400 μm culets diamonds were used with an automated pressure driver. The sample assembly was formed by a lead foil (thickness $\simeq$10 μm) and a pressure medium (Ar or NaCl) which was also used as x-ray pressure gauge. The lead foil was moved away from the diamonds surface by placing *c*-BN chips (Ar loading) or a NaCl disk (NaCl loading) on the diamonds culets to ensure thermal insulation of the sample. The sample was heated on both sides by two yttrium aluminum garnet lasers providing a maximum power of 80 W. They were slightly defocused in order to create a large heated area of $\simeq$30 μm in diameter.

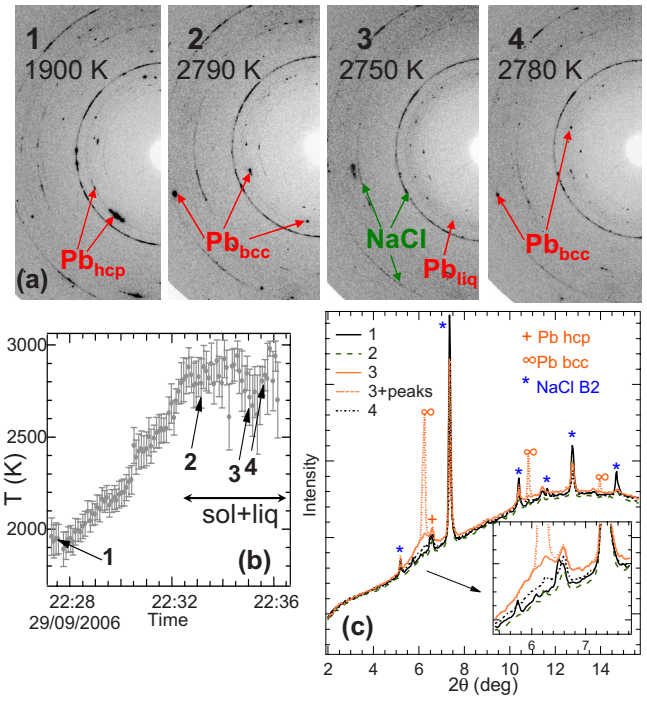

FIG. 1. (Color online) (a) Four monochromatic x-ray diffraction patterns ($\lambda=0.2647$ Å) for a {Pb+NaCl} assembly at $P=51.5$ GPa during a heating series. On the second spectrum, x-ray spots corresponding to single crystals of Pb crystallized from the melt can be seen (bcc phase); on the third and fourth spectra, the signal scattered by the melt—a diffuse ring labeled Pb_{liq}—can also be seen. (b) Corresponding temperature ramp. Laser power increases continuously with time. The temperature ramp exhibits a plateau during the solid-liquid equilibrium of lead. (c) Angularly integrated x-ray spectra. Solid x-ray diffracted spots have been hidden, except for the dotted curve that corresponds to the third spectrum. An inset is shown around the major diffuse ring.

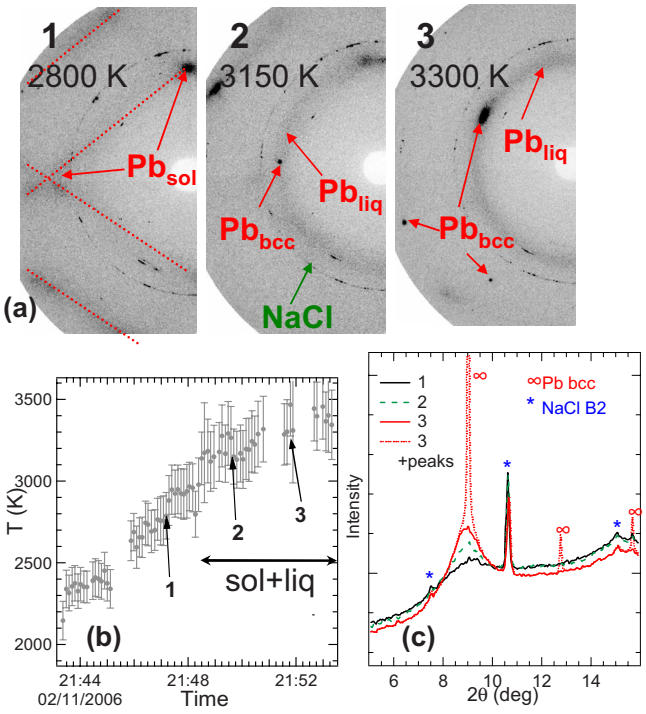

FIG. 2. (Color online) Similar patterns as in Fig. 1 at $P=65$ GPa and with $\lambda=0.3738$ Å. (a) On the first spectrum, thermal diffuse scattering by a Pb single crystal can be seen; on the second and third spectra, an additional signal scattered by the melt and x-ray spots of Pb crystallized from the melt (bcc phase) can also be seen. On the angularly integrated spectra (c), the diffuse band produced by thermal diffuse scattering of the solid and of the liquid are similar. The plateau in the temperature ramp (b) is less obvious because of the pressure drift (from 65 to 69 GPa) during solid-liquid equilibrium.

The temperature was measured at the center of the hot spot by analyzing the pyrometric signal emitted by a 2×2 μm^2 area.[23] The x-ray beam was focused on a 3×3 μm^2 area and was also aligned at the center of the hot spot (within $\simeq3$ μm) by a direct visualization on a video camera of the fluorescence signal created by the x-ray beam. This geometry was continuously checked during heating. The high x-ray flux and scattering power of lead ($Z=82$) allowed recording one diffraction spectrum on a bidimensional MarCCD detector in only $\simeq1$ s every few seconds. A second-scale crystallographic characterization of the samples has thus been performed during several heating series (gradual increase of the laser power with a record of pyrometric and diffraction spectrum every $\simeq5$ s) at different pressures.

In our experiments, most of the heating series led to the melting of the sample, evidenced by a diffuse x-ray scattered ring. Sometimes, this ring could be observed for only a few seconds. The second-scale recording of the x-ray patterns also allowed us to follow interesting and rapid changes of the sample during heating. Two different examples of these changes are presented in Figs. 1 and 2. In most of the cases, solid lead, either not molten or unsteadily crystallized from the melt, was observed at the same time as the liquid [single crystal spots appearing and disappearing on each x-ray pattern, see Fig. 1(a)]. During this liquid-solid coexistence, the sample temperature exhibited a plateau that was more or less obvious for different heating series [Figs. 1 and 2(b)]. During several heating series, fast crystallization of the sample was also observed a few minutes before the liquid diffuse ring appearance, but already on the plateau of the temperature ramp [Figs. 1(a) and 1(b)]. We interpret this fast crystallization as another sign of liquid-solid equilibrium, single crystals growing from a liquid matrix which can be detected only when its amount is sufficient to produce a clear scattered signal. At temperatures much below melting, the lead sample often recrystallized and single crystal spots, with thermal diffuse scattering,[24] could be evidenced [see Figs. 2(a) and 2(c)]. In these cases, the onset of melting was detected by checking the continuity of the diffuse ring marked as "Pb_{liq}" in Fig. 2. A chemical reaction between lead and NaCl has been observed for some heating series when hot spots had been generated (temperature higher than 4000 K).

III. MELTING CURVE

The temperature in the laser-heated sample was measured using pyrometry.[23] The error bars on measured temperature

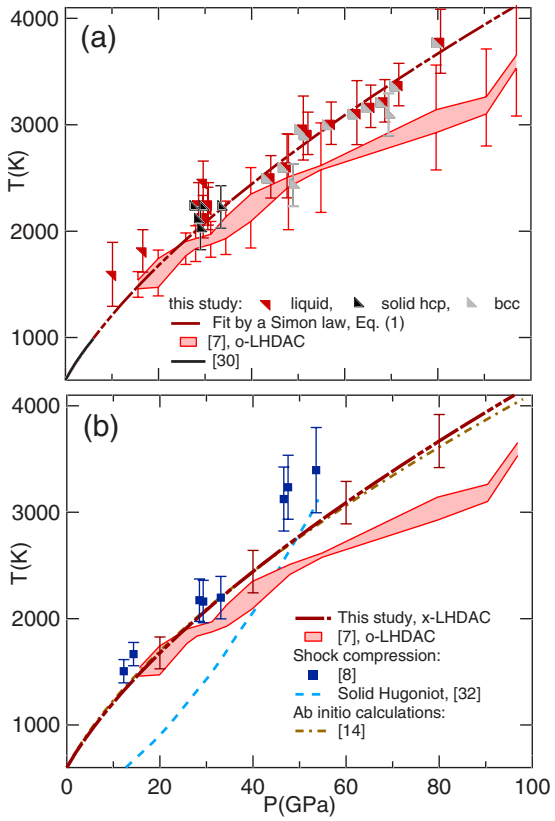

FIG. 3. (Color online) (a) Lead phases and melting curve of lead identified by x-ray diffraction (see Table I), compared to the melting curve previously obtained in o-LHDAC (Ref. 7). (b) Comparison of the melting curves predicted by *ab initio* calculations (Ref. 14) or measured by shock compression and pyrometry (Ref. 8) and LH-DAC (Ref. 7). The estimated solid Hugoniot curve (Ref. 32) is also plotted, melting being achieved around 54 GPa (Ref. 7) along this curve (end point).

(200–300 K) were estimated by comparing the results of three methods of analysis of its thermal emission spectrum recorded between ≃550 and 750 nm.[23] The pressure in the sample was estimated using the equation of state of the pressure medium. NaCl and Ar equations of state have been measured under ambient temperature[25,26] and can be estimated at high temperature using molecular dynamics[27] or a phenomenological model that includes shock-wave data.[28] Error bars ($\Delta P = \pm 4$ GPa) were obtained by assuming that the temperature in the pressure medium varies between 300 K and the temperature of the sample and taking into account the uncertainties on NaCl or Ar equations of state. Assuming that this pressure is close to the pressure in the molten sample, we obtained an estimate of the pressure in the sample higher by less than 3 GPa than the pressure after heating. This is a relatively small amount of thermal pressure, which can be explained by the high temperature stress relaxation in solids.[29]

The conditions at which solid, liquid, or liquid-solid equilibrium have been evidenced are plotted in Fig. 3(a) and listed in Table I. Our melting points are higher by ≃650 K at 80 GPa than the points obtained previously in o-LHDAC.[7] This difference is large and is similar to the error bars in Ref. 7, which evidences the major improvement from o-LHDAC to x-LHDAC technique. Our melting points can be fitted by a Simon law, together with the low pressure measurements made earlier[30] (see Fig. 3):

$$T_m = 600.6(1 + P_m/5.03)^{0.64}. \quad (1)$$

Figure 3(b) compares the melting curves of lead obtained by different approaches. The current melting curve is lower than the curve obtained by energy calculations based on an interatomic potential,[31] but in excellent agreement with molecular dynamics *ab initio* calculations of the melting of hcp phase of lead[14] and with the predictions based on the Lindemann law.[14] It has been observed that lead is molten when it is shocked at pressures higher than 54 GPa.[7] The temperature is usually not measured in shock compression experiments. In shocked solid lead, this temperature has been estimated using a phenomenological model (see Ref. 32). The resulting Hugoniot curve is plotted in Fig. 3(b). Its end point, at

TABLE I. Summary of maximum temperatures reached in each heating series, with the corresponding pressure and lead phases observed. PTM, pressure transmitting medium; S_{hcp}, hcp solid, S_{bcc}, bcc solid, L, liquid. Estimated uncertainties are 200–300 K in temperature and 4 GPa in pressure.

PTM	P (GPa)	T (K)	Phase	PTM	P (GPa)	T (K)	Phase
Ar	9.5	1580	L	NaCl	56.5	3000	$S_{bcc}+L$
Ar	29.6	2040	S_{hcp}	NaCl	62	3100	$S_{bcc}+L$
Ar	30.1	2240	$S_{hcp}+L$	NaCl	47	2600	$S_{bcc}+L$
Ar	28	2240	$S_{hcp}+L$	NaCl	49.5	2450	S_{bcc}
Ar	34	2250	S_{hcp}	NaCl	50.5	2956	$S_{bcc}+L$
NaCl	29	2446	L	NaCl	65	3160	$S_{bcc}+L$
NaCl	43.5	2497	$S_{bcc}+L$	NaCl	68	3211	$S_{bcc}+L$
NaCl	51.5	2905	$S_{bcc}+L$	NaCl	71	3363	$S_{bcc}+L$
NaCl	16	1800	L	NaCl	70	3110	S_{bcc}
NaCl	29	2122	$S_{hcp}+L$	NaCl	80	3771	$S_{bcc}+L$
NaCl	30	2200	L				

54 GPa and 3120 K, thus corresponds to a SW melting point estimated on the basis of this model.[32] The temperature of the liquid-solid equilibrium in shocked lead has also been directly measured by pyrometry at a fixed wavelength during shock release, from 54 down to 12 GPa.[8] The latter measurements are plotted in Fig. 3(b); their large error bars are due to the uncertainty on the thermal emissivity of the shocked sample. It can be seen that even if the shock melting points remain higher than the x-LHDAC melting curve, the difference between SW and static melting points is now within experimental error bars [500 K (Ref. 8) at 54 GPa]. We thus conclude that DAC and SW melting curves are now in agreement within experimental error bars.

IV. hcp-bcc PHASE TRANSITION

Before this study, the sequence of the phase transitions of lead under high pressure had been measured only under ambient temperature above 25 GPa.[33–35] The hcp and bcc high pressure phases had been observed to coexist between ≃72 and ≃200 GPa,[34,35] which suggests that the hcp→bcc transformation was kinetically hindered. The proposed pressure for the hcp-bcc transition was above 100 GPa.[34] We evidenced that the solid crystallized from the melt was the bcc phase from 44 GPa onward [see Figs. 1 and 2(c)], which locates the hcp-bcc-liquid triple point around 39±6 GPa and ≃2400 K. In their coexistence domain, the measured volumes of bcc and hcp phases are identical within experimental uncertainties, and the phase transition does not influence the Clapeyron melting slope. The hcp-bcc boundary plotted in Fig. 4 is based on the observed temperature of the hcp-bcc transformation during several heating series; above ~60 GPa, this transformation takes place at a temperature too low for a pyrometric measurement. The negative Clapeyron slope of this boundary can be explained by an entropy stabilization of the bcc phase,[36] the energies of hcp and bcc phases being very close between 50 and 150 GPa at 0 K.[37] This example demonstrates the utility of laser heating to overcome kinetic barriers and obtain the actual thermodynamically stable phases of compounds under high pressure.

V. CONCLUSION

In conclusion, the melting of lead in LHDAC has been identified by an objective x-ray based criterion, with an adapted time scale: the appearance of a diffuse x-ray scattering ring, or the fast (second scale) appearance-disappearance of lead single crystal spots. The pressure and temperature in the molten sample could be estimated with reduced error bars, and the absence of chemical reactions could be checked. We have measured a melting curve of lead that lies higher than a previous laboratory o-LHDAC measurement. x-LHDAC confirms now both SW and *ab initio* calculated melting points, solving the reported discrepancy for this element. We have also determined the stability fields of the solid phases of Pb at high pressure, with the determination of a hcp-bcc-fluid triple point at 39 GPa and 2400 K. This work thus results in a major improvement of our knowledge of the phase diagram of lead in the megabar range. Similar measurements should now be performed on other controversial systems, such as Ta or Fe, for which a spectacular difference between the extrapolated x-LHDAC melting curve and the SW data has been reported.[5,6,9] This is a necessary step before elaborating theories to explain the differences between static and dynamic measurements.

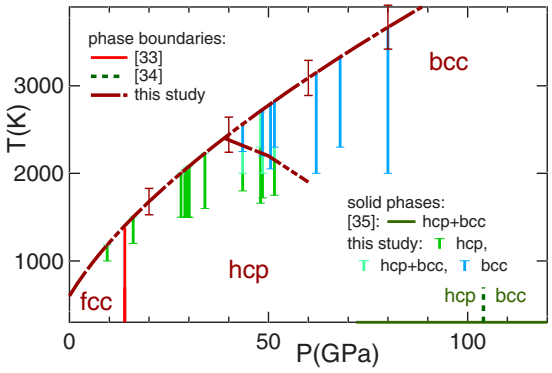

FIG. 4. (Color online) Information of the phase diagram of lead from the literature and from the current study [red (gray) dashed-dotted lines]. Reference 33, fcc→hcp transition, dotted line; Ref. 34, hcp→bcc transition at 300 K, dashed line; Ref. 35, hcp+bcc coexistence at 300 K, horizontal line. The vertical blue (gray) lines indicate the domains where hcp (dark) and bcc (light) phases have been observed during heating series in the current studies.

ACKNOWLEDGMENTS

We acknowledge the European Synchrotron Radiation Facility for provision of synchrotron radiation facilities on beamline ID27, during beam time allocated to Proposal No. HS-3159. We would like to thank several people who have a contribution to this work. R. Boehler has participated to the laser-heating setup at ESRF. C. Sortais, T. Le Bihan, and M. Cadignan helped us in preliminary experiments. P. Dorogokupets provided us an equation of state of NaCl prior to publication. We also thank D. Partouche-Sebban and J.-L. Pelissier for helpful discussions.

*Present address: Synchrotron Soleil, BP 48, 91192 Gif-sur-Yvette Cedex, France.

[1] M. Togaya, Phys. Rev. Lett. **79**, 2474 (1997); S. Brygoo, E. Henry, P. Loubeyre, J. Eggert, M. Koenig, B. Loupias, A. Benuzzi-Mounaix, and M. Rabec Le Gloahec, Nat. Mater. **6**, 274 (2007).
[2] R. Boehler, Nature (London) **363**, 534 (1993).
[3] D. Alfe, L. Vocadlo, G. Price, and M. Gillan, J. Phys.: Condens. Matter **16**, S973 (2004).
[4] S. Japel, B. Schwager, R. Boehler, and M. Ross, Phys. Rev. Lett.

95, 167801 (2005).
[5] D. Errandonea, B. Schwager, R. Ditz, C. Gessmann, R. Boehler, and M. Ross, Phys. Rev. B **63**, 132104 (2001).
[6] D. Errandonea, M. Somayazulu, D. Hausermann, and H.-K. Mao, J. Phys.: Condens. Matter **15**, 7635 (2003).
[7] B. K. Godwal, C. Meade, R. Jeanloz, A. Garcia, A. Y. Liu, and M. L. Cohen, Science **248**, 462 (1990).
[8] D. Partouche-Sebban *et al.*, J. Appl. Phys. **97**, 043521 (2005).
[9] J. H. Nguyen and N. C. Holmes, Nature (London) **427**, 339 (2004).
[10] S.-N. Luo and T. J. Ahrens, Phys. Earth Planet. Inter. **143-144**, 369 (2004).
[11] V. Sorkin, E. Polturak, and J. Adler, Europhys. Lett. **76**, 623 (2006).
[12] D. Alfè, M. J. Gillan, and G. D. Price, Nature (London) **401**, 462 (1999).
[13] S. Taioli, C. Cazorla, M. J. Gillan, and D. Alfè, Phys. Rev. B **75**, 214103 (2007).
[14] F. Cricchio, A. B. Belonoshko, L. Burakovsky, D. L. Preston, and R. Ahuja, Phys. Rev. B **73**, 140103(R) (2006).
[15] A. B. Belonoshko, R. Ahuja, and B. Johansson, Phys. Rev. Lett. **87**, 165505 (2001).
[16] A. B. Belonoshko, R. Ahuja, and B. Johansson, Nature (London) **424**, 1032 (2003).
[17] E. Gregoryanz, C. Sanloup, M. Somayazulu, J. Badro, G. Fiquet, H.-K. Mao, and R. J. Hemley, Nat. Mater. **3**, 294 (2004).
[18] J. H. Eggert, G. Weck, P. Loubeyre, and M. Mezouar, Phys. Rev. B **65**, 174105 (2002); E. Gregoryanz, O. Degtyareva, M. Somayazulu, R. J. Hemley, and H.-K. Mao, Phys. Rev. Lett. **94**, 185502 (2005).
[19] C. Sanloup, F. Guyot, P. Gillet, G. Fiquet, R. J. Hemley, M. Mezouar, and I. Martinez, Europhys. Lett. **52**, 151 (2000).
[20] G. Shen, V. B. Prakapenka, M. L. Rivers, and S. R. Sutton, Phys. Rev. Lett. **92**, 185701 (2004).
[21] M. Mezouar, W. Crichton, S. Bauchau, F. Thurel, H. Witsch, F. Torrecillas, G. Blattmann, P. Marion, Y. Dabin, J. Chavanne, O. Hignette, C. Morawe, and C. Borel, J. Synchrotron Radiat. **12**, 659 (2005).
[22] E. Schultz *et al.*, High Press. Res. **25**, 71 (2005).
[23] L. R. Benedetti and P. Loubeyre, High Press. Res. **24**, 423 (2004).
[24] A. Guinier, *X-Ray Diffraction in Crystals, Imperfect Crystals, and Amorphous Bodies* (Dover, New York, 1994).
[25] M. Ross, H.-K. Mao, P. M. Bell, and J. A. Xu, J. Chem. Phys. **85**, 1028 (1986).
[26] S. Ono, T. Kikegawa, and Y. Ohishi, Solid State Commun. **137**, 517 (2006).
[27] A. B. Belonoshko, High Press. Res. **10**, 583 (1992).
[28] P. I. Dorogokupets and A. R. Oganov, Phys. Rev. B **75**, 024115 (2007); P. I. Dorogokupets and A. Dewaele, High Press. Res. (to be published).
[29] A. Dewaele, G. Fiquet, and P. Gillet, Rev. Sci. Instrum. **69**, 2421 (1998).
[30] P. Mirwald and G. Kennedy, J. Phys. Chem. Solids **37**, 795 (1976).
[31] J.-L. Pelissier, Physica A **126A**, 271 (1984).
[32] C. Dai, H. Tan, and H. Geng, J. Appl. Phys. **92**, 5019 (2002).
[33] A. Kuznetsov, V. Dmitriev, L. Dubrovinsky, V. Prakapenka, and H. P. Weber, Solid State Commun. **122**, 125 (2002).
[34] C. A. Vanderborgh, Y. K. Vohra, H. Xia, and A. L. Ruoff, Phys. Rev. B **41**, 7338 (1990); the pressure of the hcp-bcc transition was modified according to the pressure scale by A. Dewaele, P. Loubeyre, and M. Mezouar, *ibid.* **70**, 094112 (2004).
[35] H. Mao, Y. Wu, J. Shu, J. Hu, R. Hemley, and D. Cox, Solid State Commun. **74**, 1027 (1990).
[36] R. E. Watson and M. Weinert, Phys. Rev. B **30**, 1641 (1984).
[37] A. Y. Liu, A. Garcia, M. L. Cohen, B. K. Godwal, and R. Jeanloz, Phys. Rev. B **43**, 1795 (1991).